Tetrahedron 67 (2011) 9104–9111

Contents lists available at SciVerse ScienceDirect

Tetrahedron

journal homepage: www.elsevier.com/locate/tet

Oxazolidinone cross-alkylation during Evans' asymmetric alkylation reaction

Nieves Fresno [a], Ruth Pérez-Fernández [a,*], Pilar Goya [a], Mª Luisa Jimeno [a], Ibón Alkorta [a], José Elguero [a], Laura Menéndez-Taboada [b,*], Santiago García-Granda [b]

[a] Instituto de Química Médica, IQM-CSIC, Juan de la Cierva, 3, E-28006 Madrid, Spain
[b] Departamento de Química Física y Analítica, Facultad de Química, Universidad de Oviedo, Julián Clavería, 8, E-33006 Oviedo, Spain

ARTICLE INFO

Article history:
Received 21 July 2011
Received in revised form 16 September 2011
Accepted 20 September 2011
Available online 25 September 2011

Keywords:
Oxazolidinone
Asymmetric alkylation
X-ray crystallography
Multinuclear NMR
DFT calculations

ABSTRACT

Starting from Evans' imidazolidin-2-one (**1**) two compounds were obtained by *trans*-N-acylation: the expected one **3** with *S*,*R* configuration and a second compound **5**, that is, related to **3** by the loss of a $CH(CH_3)C{=}O$ fragment. The stereochemistry of **3** was established by NMR spectroscopy, mainly NOE experiments, as expected, the new center has an S configuration, the compound being thus *S*,*R*. The structure of compound **5** was determined by X-ray crystallography. A mechanism of formation of **5** was proposed.

© 2011 Elsevier Ltd. All rights reserved.

1. Introduction

Compounds with an oxazolidine ring are of major interest because of their presence in several biologically active synthetic products. Oxazolidin-2-ones are amongst the very few genuinely new antimicrobial classes developed in the past 30 years, being linezolid[1,2] (Fig. 1) the only one marketed so far. Besides, their usefulness as directing groups in asymmetric synthesis has been fully tested. In the 1980s, Evans et al.[3] and Masamune et al.[4] reported a series of chiral auxiliaries bearing an oxazolidine ring in asymmetric reactions that proceeded with high stereoselectivity.

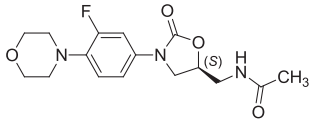

Fig. 1. Linezolid structure.

The asymmetric alkylation reactions arouse interest from a synthetic, mechanistic, and theoretical point of view. The development of *N*-acyl oxazolidinones as chiral enolate synthons in carbon–carbon bond forming reactions has exhibited high levels of diastereoselectivity in alkylation reactions.

In early studies, it was shown that either lithium or sodium hexamethyldisilazide bases (1.1 equiv of $LiN[Si(CH_3)_3]_2$ or $NaN[Si(CH_3)_3]_2$), transformed imides to their respective *Z*-metal enolates creating a diaestereofacial bias in the alkylation process with more than 97% ee.[5,6] This comes as a result of combining the ability of acylated oxazolidinones to chelate to metal ions and the steric hindrance caused by suitable substituents (R=Bn, $CHMe_2$) at the 4 position of the ring, in this case *R* has an *R* absolute configuration (Scheme 1).

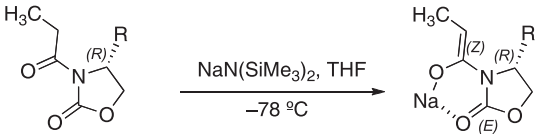

Scheme 1. Preparation of *Z*-metal enolates from (*R*)-(−)-4-substituted-3-propionyl-2-oxazolidinones.

Nomura et al. have reported their observations of Evans' asymmetric alkylation methodology in the synthesis of a selective agonist for human peroxisome proliferator-activated receptor alpha (PPARα).[7] They stated that the sodium enolate derivative of their oxazolidinones were less stable at temperatures above −78 °C than the corresponding lithium derivative, but with no mention to any byproducts.

Some years earlier, parallel studies reported on the development of a new class of chiral auxiliaries, the 5,5-substituted SuperQuats, while focusing on up-scaling. The asymmetric

* Corresponding authors. Tel.: +34 91 562 2900; fax: +34 91 564 4853 (R.P.-F.); tel.: +34 985 102 966; fax: +34 985 103 125 (L.M.-T.); e-mail addresses: rperezf@iqm.csic.es (R. Pérez-Fernández), menendezlaura.uo@uniovi.es (L. Menéndez-Taboada).

0040-4020/$ – see front matter © 2011 Elsevier Ltd. All rights reserved.
doi:10.1016/j.tet.2011.09.083

alkylations with SuperQuat auxiliaries using LiHMDS at −78 °C revealed the existence of byproducts with variable yields depending on the SuperQuat derivative used.[8]

2. Results and discussion

The purpose of this paper is to report our observations on the effects of the organic base and temperature regarding Evans' asymmetric alkylation preparing chiral α-methylphenylmetanoic acid derivatives from acyl oxazolidinones (R=Bn, $CHMe_2$) and methyl 3-bromomethyl benzoate. The effects of the organic base (LiHMDS, NaHMDS, KO^{t}Bu) in a range of temperatures from −78 °C to room temperature on the reaction of oxazolidinones **1** and **2** with benzyl 3-bromomethyl benzoate was explored.

At first, 1.1 equiv of NaHMDS (1.0 M in THF) were added to a solution of oxazolidinone **1** in THF at −78 °C. Thirty minutes after the start of the reaction, methyl 3-bromomethyl benzoate was slowly added. The reaction was completed in 6 h yielding the desired (*S*)-configuration product, (*S*,*R*)-**3**, with 95% ee (Scheme 2).[9]

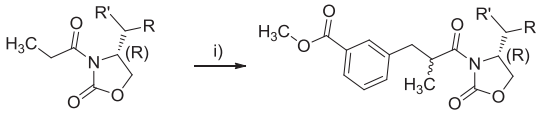

Scheme 2. Synthesis of compounds **3** and **4**. Reagents and conditions: (i) NaHMDS 1.0 M in THF, methyl 3-bromomethyl benzoate, THF dry, −78 °C, 7 h.

When 1.1 equiv of LiHMDS (1.6 M in THF) were used instead of NaHMDS at −78 °C, compounds (*S*,*R*)-**3** and (*S*,*R*)-**4** were obtained in very low yields. Subsequently, the reaction at −20 °C was attempted expecting the corresponding lithium enolate derivative of the oxazolidinones to be more stable at higher temperatures than the sodium enolate one, but surprisingly the final compounds (*S*,*R*)-**3** and (*S*,*R*)-**4** were also obtained in very low yields.

From a practical point of view it was not convenient to perform reactions at a very low temperature. We looked for a base that could work at room temperature like the potassium *tert*-butoxide. In a similar fashion the reactions were set up this time using 1 equiv of KO^{t}Bu and changing the reaction temperature to room temperature.

Unexpectedly, the major product of the reaction was compound **5** obtained with a 62% yield (Scheme 3). The loss of the propionic group was confirmed with NMR experiments and X-ray crystallographic analysis of the structure.

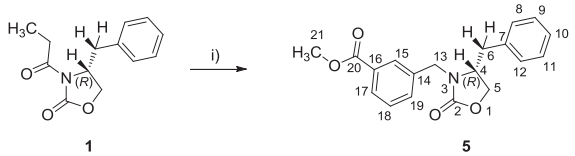

Scheme 3. Synthesis of compound **5** from **1**. Reagents and conditions: (i) *t*-BuOK, Methyl 3-bromomethyl benzoate, THF dry, 7 h.

2.1. Determination of the stereochemistry of compound 3

The synthesis of **3** (Scheme 2) affords a unique compound with the benzyl group of the oxazolidinone in a (*R*) configuration, corresponding to that of the starting **1**, and an unknown configuration of the methyl group of the lateral chain (Scheme 4). According to the synthetic methodology used, the second center should be (*S*), obtaining **3** (*S*,*R*).

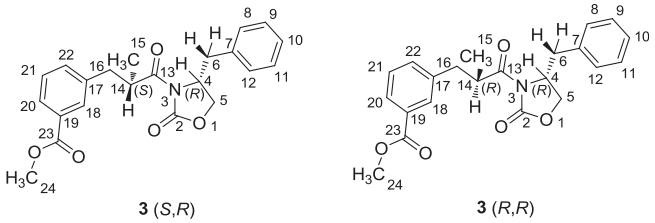

Scheme 4. The two diastereoisomers of compound **3**.

To establish independently the relative configuration of the methyl group at 14-position, we have carried out B3LYP/6-311++G(d,p) calculations. One of the minimum energy conformations has an extended geometry (Fig. 2) being the (*S*,*R*) diastereoisomer 0.95 kJ mol^{-1} more stable than the (*R*,*R*) one, but this is irrelevant since the stereochemistry of the new center is of kinetic origin. To avoid cumbersome discussions we will assume that the compound has the (*S*,*R*) configuration.

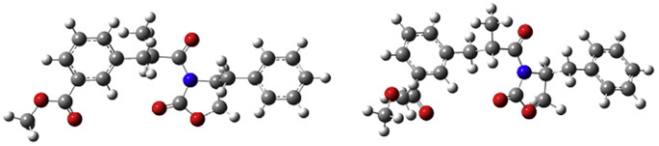

Fig. 2. Minimized structures of compound **3** [B3LYP/6-311++G(d)]: left 14(*S*),4(*R*), right 14(*R*),4(*R*).

We have used these geometries to calculate the chemical shifts of both diastereoisomers (from the absolute shieldings calculated at the GIAO approximation). They are very similar, preventing any assignment (Table 1). We have reported the chemical shifts for the ^{13}C NMR spectrum (at 75.47 MHz) and the chemical shifts and ^{1}H–^{1}H coupling constants for the ^{1}H NMR spectrum (at 499.98 MHz). For the aromatic protons only the chemical shifts are reported (first order analyzed) but the two saturated fragments (Me15–H14–H16$_a$–H16$_b$) and (H5$_a$–H5$_b$–H4–H6$_a$–H6$_b$) were iteratively analyzed. It is not the aim of this paper to carry out a conformational analysis of compound **3**, thus we have used the ^{13}C calculated chemical shifts of **3**(*S*,*R*) together with 2D experiments to assign the experimental signals (Table 1). From ^{13}C we have assigned unambiguously all the ^{1}H attached to a given carbon atom, including the equivalent *ortho* and *meta* carbons at 8, 9, 11, and 12 positions.

The only assignments that remain concern are the methylene protons at 5, 6, and 16 positions.

Concerning the ring fragment C4C5, we have calculated the spin–spin coupling constants (SSCC) of the model compounds reported in Fig. 2 at the B3LYP/6-311++G(d,p) level optimizing previous B3LYP/6-31G(d) optimizations (frequencies were calculated to verify that they were minima). Since the oxazolidin-2-one ring is not planar, there could be a fast ring flipping[12–14] and the experimental SSCC should be compared to the average ones (Fig. 3).

The agreement is acceptable providing an assignment of H5$_a$ [4.181 ppm, ^3J=8.03 (H4)] and H5$_b$ [4.117 ppm, ^3J=2.89 (H4)].

The $^3J_{HH}$ coupling constants and the Karplus equation[15–17] were used to check if the torsion angles of the optimized (*S*,*R*) structure agreed with those deduced from the Karplus equation. The optimized structure calculated (top of Table 1) was one example among the different possibilities. For going from $^3J_{vic}$ SSCC to torsion angles we have used the software created by Navarro-Vázquez et al. that takes into account the substituents linked to the different C–C fragments, in our case CH_3 (instead of CH_2Ph), $CONH_2$ (instead of N–CO–R), Ph, and CH_2OR (instead of CH_2–O-ring).[18] We have calculated several conformations and adjusted the populations to reproduce the SSCC.

Table 1
Experimental (^{1}H at 499.88 MHz and ^{13}C at 75.47 MHz) and calculated ^{1}H and ^{13}C chemical shifts of compound **3** *S,R*

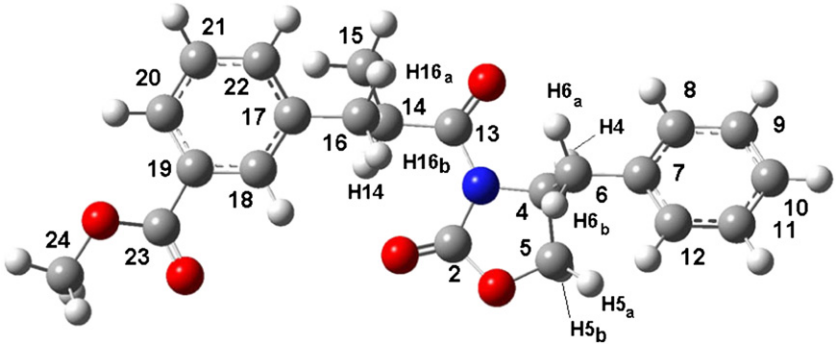

Atom	Experimental chemical shifts	Experimental coupling constants	*S,R* calculated chemical shifts	*R,R* calculated chemical shifts
^{1}H				
H4	4.670	^3J=9.46 (H6$_a$) ^3J=8.03 (H5$_a$) ^3J=3.41 (H6$_b$) ^3J=2.89 (H5$_b$)	4.35	4.38
H5$_a$	4.181	^2J=−9.17 (H5$_b$) ^3J=8.03 (H4) ^4J=0.68 (H6$_a$)[a,b]	3.89	3.84
H5$_b$	4.117	^2J=−9.17 (H5$_a$) ^3J=2.89 (H4)	4.09	4.03
H6$_a$	3.123	^2J=−13.45 (H6$_a$) ^3J=3.41 (H4) ^4J=0.68 (H5$_a$)[a]	3.45	3.53
H6$_b$	2.573	^2J=−13.45 (H6$_b$) ^3J=9.46 (H4)	2.38	2.37
H8, H12 (*ortho*)	7.05	—	7.36	7.38
H9, H11 (*meta*)	7.26	—	7.33	7.34
H10 (*para*)	7.26	—	7.30	7.24
H14	4.107	^3J=7.02 (CH$_3$) ^3J=7.16 (H16$_a$) ^3J=7.33 (H16$_b$)	3.75	3.99
H15 (CH$_3$)	1.193	^3J=7.02 (H14)	0.92	0.93
H16$_a$	2.729	^2J=−13.46 (H16$_b$) ^3J=7.16 (H14)	2.10	3.18
H16$_b$	3.207	^2J=−13.46 (H16$_a$) ^3J=7.33 (H14)	3.40	2.18
H18	7.93	—	8.76	8.74
H20	7.90	—	7.94	7.96
H21	7.37	—	7.17	7.10
H22	7.51	—	7.22	7.18
H24 (CH$_3$)	3.87	singlet	3.76	3.73
^{13}C				
C2 (C=O)	153.45	—	151.39	151.49
C4	55.58	—	59.47	59.86
C5	66.40	—	65.14	64.67
C6	38.21	—	38.56	38.86
C7	135.55	—	137.99	138.34
C8, C12 (*ortho*)	129.76	—	129.22	129.08
C9, C11 (*meta*)	129.33	—	128.82	129.00
C10 (*para*)	127.74	—	127.08	126.58
C13 (C=O)	176.60	—	175.57	175.83
C14	39.98	—	43.77	43.84
C15 (CH$_3$)	17.13	—	13.25	12.87
C16	39.92	—	41.98	43.17
C17	139.98	—	141.18	141.28
C18	130.81	—	132.36	132.49
C19	139.67	—	131.23	131.20
C20	128.89	—	128.08	127.92
C21	128.23	—	126.72	127.06
C22	134.37	—	134.53	133.97
C23 (C=O)	167.49	—	166.04	164.63
C24 (CH$_3$)	50.94	—	50.95	52.65

[a] Note that protons H5$_a$ and H6$_b$ are coupled (^4J=0.68 Hz) due to their W or M pattern (H–C–C–C–H).[10]
[b] The coupling on this signal is difficult to measure due to the benzylic $^4J_{HH}$ coupling constant of similar magnitude (for benzylic coupling constants see Ref. 11).

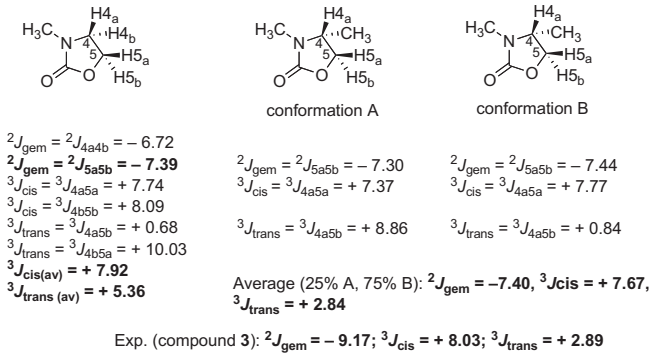

Fig. 3. Calculated and experimental coupling constants for the C4C5 fragment.

(i) Fragment C14–C16 ($CHMe–CH_2$). We have measured two $^3J_{vic}$ (Table 1) of H14 with $H16_a$ (7.16 Hz) and $H16_b$ (7.33 Hz), the corresponding dihedral angles ϕ being 178.9° and 62.3° according to the optimized structure (Fig. 2, **3** *S*,*R*). Assuming two other staggered structures obtained from this one and rotating about the C14–C16 bond by 120 and 240°, three conformations were obtained (Scheme 5).

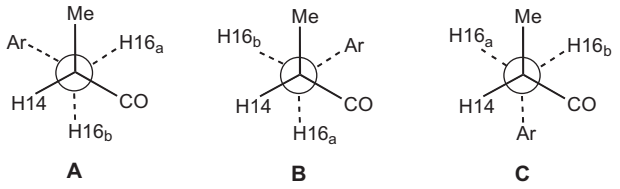

Scheme 5. The three staggered conformations of compound **3** about the C14–C16 bond.

The calculated Karplus values of 12.85 and 3.58 Hz corresponded to an optimized conformation **A**, conformation **B** corresponded 2.80 and 3.17 Hz, and to conformation **C** corresponded the calculated Karplus values of 3.97 and 12.86 Hz. A linear model led to the following values, 40% of **A**, 20% of **B**, and 40% of **C**.

(ii) Fragment C4C5 ($CHRCH_2$) of the oxazolidin-2-one. Two very different vicinal coupling constants, 8.03 ($H4H5_a$) and 2.89 Hz ($H4H5_b$) related to 22.8 and 102.5° in the optimized geometry were measured. But, as it was shown in Fig. 3, there could be another conformation corresponding to the ring inversion (Scheme 6). This conformation was optimized independently and it resulted to be less stable.

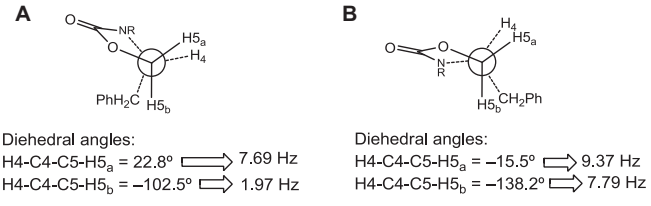

Scheme 6. The two flipped conformations of compound **3** about the C4–C5 bond.

There is no doubt that the proton with the larger coupling corresponds to $H5_a$ at 4.181 ppm. Using the Karplus equation the four calculated values of Scheme 6 were 82% of **A** (that of our optimized structure) and 18% of **B**.

The fact that $H5_a$ (4.181 ppm) is coupled with $H6_a$ with a ^4J_W=0.68 Hz has being essential for the assignment of $H6_a$ and $H6_b$ (see iii).

(iii) Fragment C4–C6 ($CHring–CH_2$). The two coupling constants of 9.46 Hz (2.573 ppm) and 3.41 (3.123 ppm) together with the ^4J_W=0.68 Hz (with $H5_a$) belongs to this fragment. The following Karplus calculated coupling constants correspond to the three conformations of Scheme 7, **A** (3.69 and 11.89 Hz), **B** (2.53 and 3.43 Hz), and **C** (11.98 and 2.79 Hz). A linear model led to the following values 71% of **A** (that corresponded to our minimized geometry), 29% of **B**, and 0% of **C**.

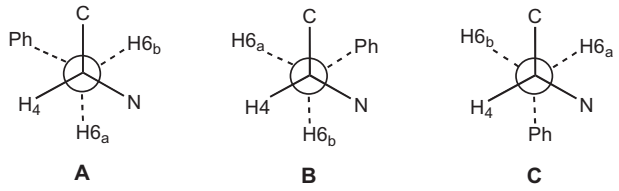

Scheme 7. The three staggered conformations of compound **3** about the C4-C6 bond.

In conclusion, the calculated minimum energy conformation is only one of the minima in a complex surface.

Taking into account the conformations deduced from the Karplus equation, it appears that the relative configuration of the C14 atom (15-methyl group position and H14), could be established by selective NOE experiments with the CH_2 at 6 position. Table 2 summarized the results of the NOE selective experiments. From these experiments it is clear that the stereochemistry of C14 is (*S*) confirming the stereochemistry of **3** as (*S*,*R*).

Table 2
Selective NOE experiments

Irradiated signal	Chemical shift	Affected signal	Unaffected signal
Methyl group, H15	1.193	4.107 (H14)	3.123 ($H6_a$)
		3.207 ($H16_b$)	2.573 ($H6_b$)
		2.729 ($H16_a$)	
		7.51 (H22)	
		7.93 (H18)	
H6a	3.123	4.670 (H4)	1.193 (Me15)
		4.107 (H14)	
		2.573 ($H6_b$)	
		7.05 (*Hortho*, H8, H12)	
		7.93 (H18)	
H4	4.670	2.573 ($H6_b$)	1.193 (Me15)
		3.123 ($H6_a$)	
		4.181 ($H5_a$)	
		7.05 (*Hortho*, H8, H12)	

2.2. Determination of the structure of compound 5

Compound **5** gave crystals suitable for X-ray analysis. The molecular structure of compound **5** is represented projected along the *a*-axis in Fig. 4 (left) while the unit-cell view down *a*-axis is shown in Fig. 4 (right).

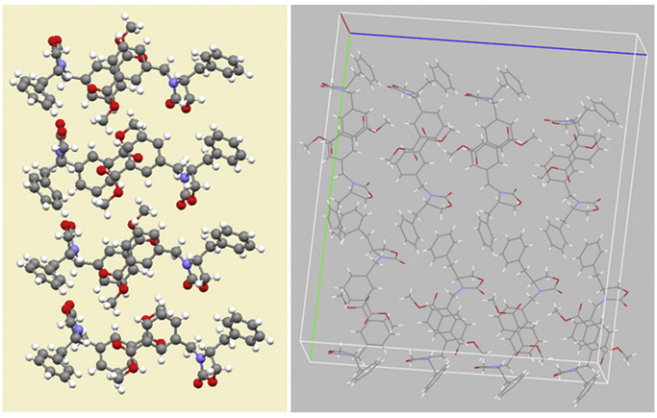

Fig. 4. View of compound **5** along the *a*-axis (left) and its unit cell (right).

Crystal packing views are shown in Figs. 5 and 6. The single crystal X-ray structure data are listed in Table 3. Hydrogen-bonding geometry is presented in Table 4.

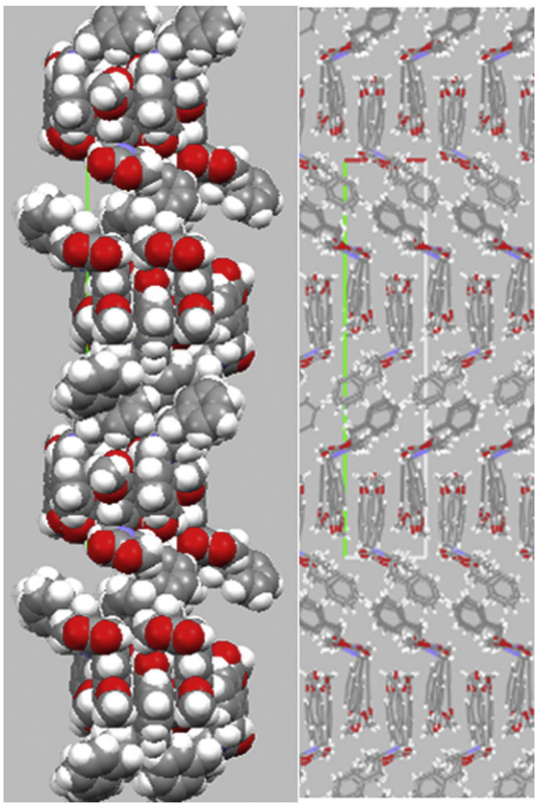

Fig. 5. Crystal packing. View along *c*.

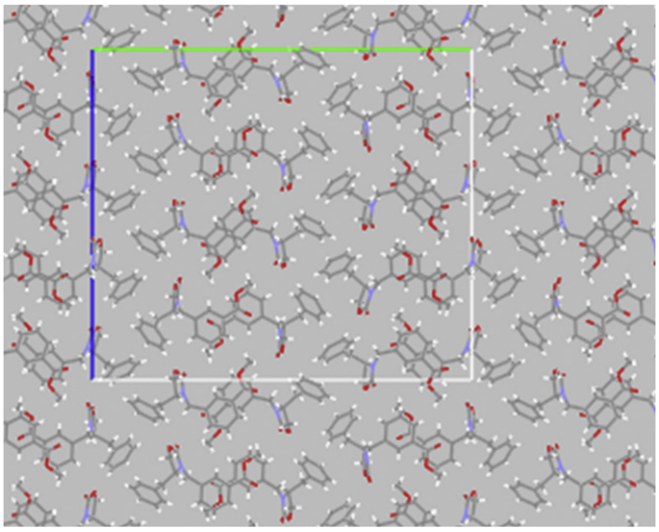

Fig. 6. Crystal packing. View along *a*.

As shown in Fig. 7 the crystal packing of compound **5** shows chains along *a* crystallographic axis formed by hydrogen bonds (–C–H···O=C–). Chains are stabilized by very weak π–π interactions between aromatic rings within the chain, but according to centroid–centroid distances between two aromatic rings and the angles between the normal of the benzene ring and the centroid vector, only π–π stacking interaction can be justified in one of the four pairs of centroids. –H–π interactions between these chains

Table 3
Crystal data and structure refinement for compound **5**

Compound **5**	
Empirical formula	C19 H19 N O4
Formula weight	325.35
Temperature (*K*)	100
Wavelength (Å)	1.54184
Crystal system	Monoclinic
Space group	$P2_1$
a (Å)	7.0958(1)
b (Å)	32.9935(6)
c (Å)	28.2202(5)
β (°)	90.377(2)
b (Å)	32.9935(6)
Z	16
μ (mm^{-1})	0.753
F(000)	2752
Crystal size (mm)	0.51×0.25×0.07
Reflections collected	47,287
Unique reflections	23,654
R(int)	0.0340
$R_1[I>2\sigma(I)]$	0.0401
wR_2 (all data)	0.1015
Absolute structure parameter	0.09(9)

Table 4
Hydrogen-bond geometry (Å, °)

D–H···A	D–H	H···A	D···A	D–H···A
C31–H31···O2[a]	0.98	2.25	3.227 (3)	176
C126–H126···O14	0.98	2.27	3.253 (3)	176
C12–H12···O6	0.98	2.31	3.291 (3)	174
C69–H69···O26[a]	0.98	2.32	3.293 (3)	174
C107–H107···O18	0.98	2.57	3.511 (3)	160
C15–H15···Cg6[b]	0.93	2.64	3.563 (3)	171
C114–H114···Cg9[b]	0.93	2.71	3.637 (3)	175
C53–H53···Cg21[c]	0.93	2.86	3.778 (3)	171
C34–H34···Cg18[c]	0.93	2.59	3.505 (3)	167
C72–H72···Cg24[d]	0.93	2.57	3.472 (3)	163
C133–H133···Cg12[e]	0.93	2.58	3.469 (3)	161
C142–H30*B*···Cg24[f]	0.97	2.95	3.799 (3)	147

Symmetry codes.
[a] *x*−1, *y*, *z*.
[b] −*x*+1, *y*−1/2, −*z*+1.
[c] −*x*+1, *y*+1/2, −*z*+1.
[d] −*x*, *y*+1/2, −*z*+1.
[e] −*x*+1, *y*−1/2, −*z*.
[f] *x*+1, *y*, *z*.

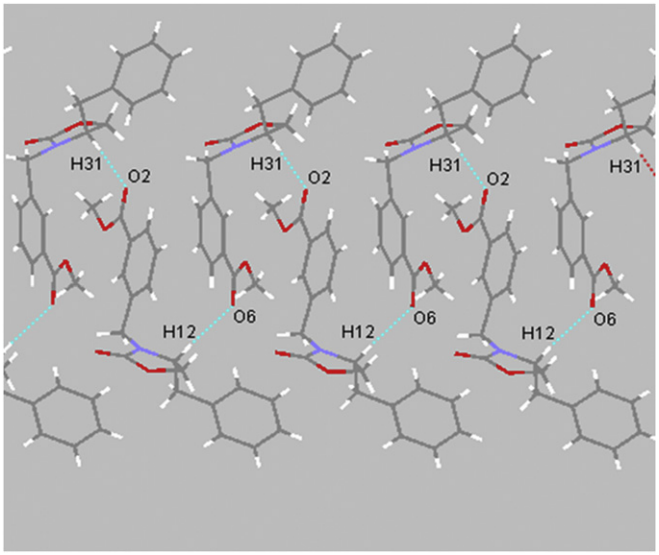

Fig. 7. Hydrogen bonds in compound **5** (C(12)–H(12)···O(6) y C(31)–H(31)···O(2)). Chains along *a*. View along *c*.

also contribute to the crystal packing forming layers along *b* crystallographic axis (Figs. 8 and 9).

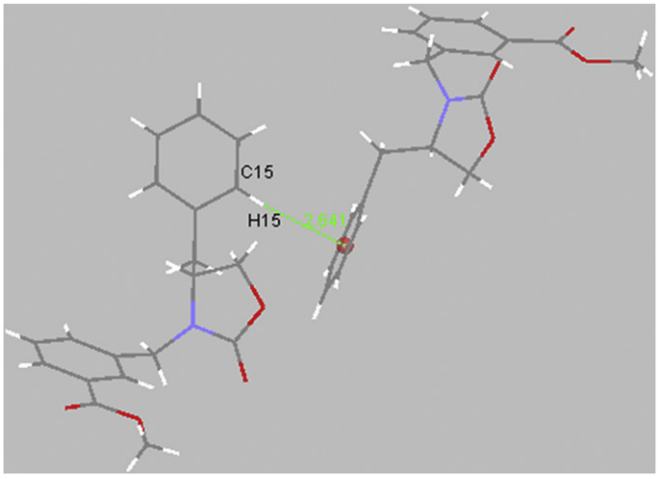

Fig. 8. H–π interaction (C15–H15···Cg6).

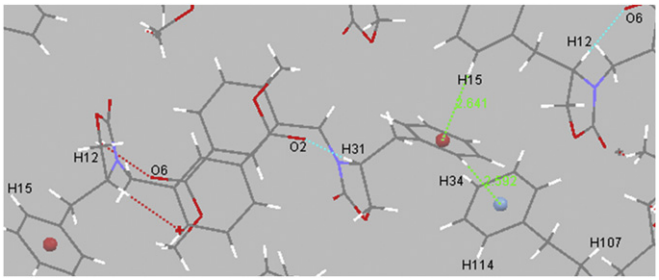

Fig. 9. H–π interaction (C15–H15···Cg6 and C34–H34···Cg18), forming layers along *b*.

The crystal packing of compound **5** shows chains along *a* crystallographic axis, formed by hydrogen bonds (–C–H···O=C–), as shown in Fig. 7. Chains are stabilized by very weak π–π interactions between aromatic rings within the chain, but according to centroid–centroid distances between two aromatic rings and the angles between the normal of the benzene ring and the centroid vector, only π–π stacking interaction can be justified in one of the four pairs of centroids. –H–π interactions between these chains also contribute to the crystal packing forming layers along *b* crystallographic axis (Figs. 8 and 9) (Table 5).

Table 5
π–π interactions (Å, °, *J*). Where Alpha=dihedral angle between planes *I* and *J*, Beta=Angle Cg(*I*)→Cg(*J*) or Cg(*I*)→Me vector and normal to plane *I*, Gamma=angle Cg(*I*)→Cg(*J*) vector and normal to plane *J* (°) and Cg–Cg=distance between ring centroids

Cg(*I*)	Cg(*J*)	d Cg–Cg	Alpha	Beta	Gamma	Symmetry code
Cg(5)	≥ Cg(2)	3.8720(14)	13.2493	13.09(11)	24.11	*x*, *y*, *z*

The NMR spectrum of five in $CDCl_3$ solution is reported in the experimental part being fully consistent with the proposed structure.

Since compound **5** crystallizes with $Z'=6$ we decided to record its ^{13}C and ^{15}N CPMAS NMR spectra by analogy with camphopyrazole,[19,20] a compound with $Z'=6$ where all the signals were split up to six peaks. Unfortunately, no splitting was observed in any case.

The reaction mechanism of this cross-alkylation is thought to be as follows: first the potassium *tert*-butoxide deprotonates the alpha-hydrogen. Upon addition of the bromide derivative the enolate gives rise to the ketene and the concomitant oxazolidinone anion attacks the benzyl bromide derivative (Scheme 8).

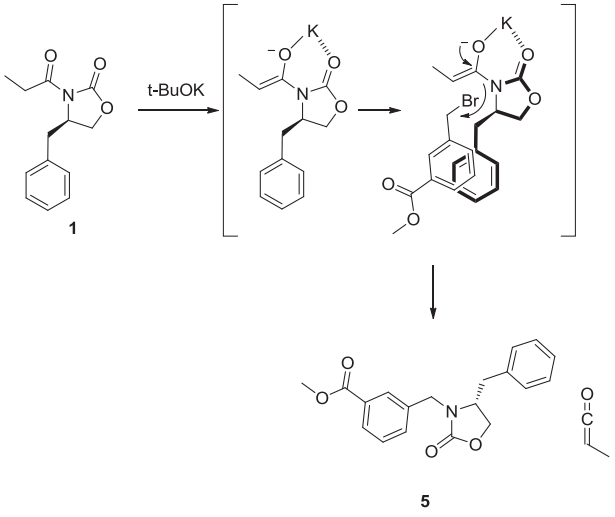

Scheme 8. Proposed mechanism for the **1** to **5** transformation.

3. Conclusions

The reaction of (*R*)-(–)-4-benzyl-3-propionyl-2-oxazolidinone with methyl 3-bromomethyl benzoate in basic medium afforded two different compounds, **3** and **5**, depending on the experimental conditions. Both products were identified by NMR, MS and, one of them (**5**), by X-ray crystallography. Compound **3** is a useful intermediate in the design of PPAR (Peroxisome Proliferator-Activated Receptor) ligands,[7,21] whereas compound **5** has been found as substructure in cholesteryl ester transfer protein (CETP) inhibitors, such as Anacetrapib.[22,23] Both structures could be developed into bioactive ligands to treat metabolic disorders.

4. Experimental section

4.1. General

All chemicals were purchased from commercial suppliers and used without further purification. TLC: precoated silica-gel 60 254 plates (Merck), detection by UV light (254 nm). Flash-column Chromatography (FC): Kieselgel 60 (230–400 mesh; Merck). Melting points (mp) were determined in open capillaries with a Gallenkamp capillary melting-points apparatus and are uncorrected. ^1H and ^{13}C NMR spectra were recorded on Bruker Advance 300 spectrometer operating at 300.13 MHz and 75.47 MHz, respectively, in $CDCl_3$ as solvent. In the case of the ^1H NMR spectrum of **3** in $CDCl_3$ we record the spectrum a Varian Inova 400 NMR spectrometer, equipped with a 5-mm broadband probe, operating at 399.90 MHz. Chemical shifts are reported in parts per million on the δ scale. In the case of multiplets, the signals are reported as intervals. Signals were abbreviated as s, singlet; d, doublet; t, triplet, and m, multiplet. Coupling constants are expressed in hertz. ROESY spectrum was obtained using the Varian standard pulse sequence with a mixing time of 200 ms. For this spectrum, 32 transients were collected for each of 200 increments in F1. The data were processed with Gaussian apodizations in each dimension and backward linear prediction was applied in F1 followed by DC corrections. NOESY1D spectra were collected employing a homospoil gradient pulse for randomization of magnetization prior to the relaxation delay. Sech180 shaped pulses were used for selective excitation of specific resonances. LC-MS analyses were performed

using an Alliance 2695 (Waters) with a diode array UV–vis detector Waters 2996 and interfaced to a Micromass ZQ mass spectrometer. Analyses were performed using reversed phase HPLC silica based columns: Sunfire™ C 18 3.5 μm (4.6×50 mm). Using an injection volume of 10 μL, a flow rate of 1 mL/min and gradient elution (5–95% over 18 min) or (10–100% over 5 min) of acetonitrile in water. Acetonitrile contains 0.08% v/v and water contains 0.1% v/v formic acid. Analyses were monitored at 254 nm wavelength.

4.2. Synthesis of methyl 3-[(*S*)-3-((*R*)-4-benzyl-2-oxooxazolidin-3-yl)-2-methyl-3-oxopropyl]benzoate (3)

A solution of (*R*)-(−)-4-benzyl-3-propionyl-2-oxazolidinone (500 mg, 2.15 mmol) in anhydrous THF (11 mL) was stirred for 15 min under nitrogen atmosphere at −78 °C. Then sodium bis(-trimethylsilyl)amide 1.0 M in THF (2.36 mL, 2.36 mmol) was added dropwise with a syringe to the stirred solution. The reaction mixture was allowed to stir for 1 h at −78 °C. Methyl 3-bromomethyl benzoate (541 mg, 2.3 mmol) was added and the reaction stirred at this temperature for 6 h. After reaching room temperature a saturated solution of NH_4Cl (15 mL) was added and the reaction extracted with ethyl acetate (30 mL). The combined organic extracts were washed successively with water (30 mL), brine (30 mL), and dried over Na_2SO_4. The solvent was evaporated and the crude purified by silica column chromatography (hexane/ethyl acetate 6:4 v/v) yielding a white solid (432 mg, 62%). Mp 98 °C. LC-MS rt=5.4, *m*/*z*: 382 (100%) $[M+H]^+$. Elemental analysis calcd for $C_{22}H_{23}NO_5$% C, 69. 28; H, 6.08; N, 3.67; found C, 69.36; H, 5.87; N, 3.94.

NMR simulations. All measurable chemical shifts and couplings constants for compound **3** were obtained from the experimental ^1H spectrum. Chemical shifts and coupling constants, measured for the two saturated fragments (Me15–H14–$H16_a$–$H16_b$) and ($H5_a$–$H5_b$–H4–$H6_a$–$H6_b$), were then submitted (negative values for the geminal couplings and positive values for the vicinal couplings) to a spectral simulation and optimization program (gNMR5.0, IvorySoft, UK)[24] that obtained a complete set of optimized values by comparing experimental with simulated spectra.

For the two former fragments, dihedral angles were obtained from the optimized coupling constants values by using the Haasnoot-de Leeuw-Altona equation for three substituents (HLA), as implemented in the Mestre-J program. However, the interpretation of vicinal coupling constants in terms of a unique dihedral angle can be complicated by conformational mobility since coupling constants may be time averages over multiple conformations. In those cases we used a rotameric model and the vicinal coupling constants were estimated for all the conformers from the corresponding dihedral angles of the calculated conformers. Finally, populations of the conformers were calculated solving systems of linear equations using the Choleski method.[25]

Reduced→Convent		Input→Reduced		T=Input→Convent: $a'=T\times a$
$\begin{pmatrix}-1&0&0\\0&0&-1\\0&-1&0\end{pmatrix}$	×	$\begin{pmatrix}-1&0&0\\0&0&-1\\0&-1&0\end{pmatrix}$	=	Det (T) 1.000

Cell lattice	*a*	*b*	*c*	Alpha	Beta	Gamma	Volume	Crystal system	Laue
Input mP	7.096	32.993	28.220	90.00	90.38	90.00	6607	Monoclinic	2/m
Reduced mP	7.096	28.220	32.993	90.00	90.00	90.38	6607		
Convent mP	7.096	32.993	28.220	90.00	90.38	90.00	6607	Monoclinic	2/m

Space group=*P*21
-No obvious space group change needed/suggested.

4.3. Synthesis of (*R*)-methyl.3-[(4-benzyl-2-oxooxazolidin-3-yl)methyl]benzoate (5)

To a solution of (*R*)-(−)-4-benzyl-3-propionyl-2-oxazolidinone (1200 mg, 5.24 mmol) in anhydrous THF (13 mL) was added potassium *tert*-butoxide (600 mg, 5.24 mmol) and stirred for 45 min under nitrogen atmosphere at room temperature. Then methyl 3-bromomethyl benzoate (1000 mg, 4.36 mmol) was added to the stirred solution. The reaction mixture was stirred for 6 h. A saturated solution of NH_4Cl (15 mL) was added and the reaction extracted with ethyl acetate (30 mL). The combined organic extracts were washed successively with water (30 mL), brine (30 mL) and dried over Na_2SO_4. The solvent was evaporated and the crude purified by silica column chromatography (hexane/ethyl acetate 7:3 v/v) yielding a white solid (432 mg, 62%). Mp 62 °C. LC-MS rt=4.8, *m*/*z*: 326 (100%) $[M+H]^+$. Anal. Calcd for $C_{19}H_{19}NO_4$% C, 70.14; H, 5.89; N, 4.31; found C, 70.31; H, 5.67; N, 4.60. ^1H NMR (300 MHz, $CDCl_3$) δ 8.06–7.95 (m, $1H_{Ar}$), 7.90 (s, $1H_{Ar}$), 7.54–7.40 (m, $2H_{Ar}$), 7.36–7.22 (m, $3H_{Ar}$), 7.12–7.02 (m, $2H_{Ar}$), 4.86 (d, 1H), 4.18 (m, 2H), 4.10–4.02 (m, 1H), 3.93 (s, 3H), 3.89–3.77 (m, 1H), 3.09 (dd, J_{ab}=13.6, J_{a4}=4.7 Hz, $1H_{CH2-Ar}$), 2.66 (dd, J_{ba}=13.6, J_{b4}=8.9 Hz, $1H_{CH2-Ar}$). ^{13}C NMR (75 MHz, $CDCl_3$) δ 166.5 (C20), 157.9 (C2), 136.4 (C7), 135.4 (C14), 132.4 (C19), 130.8 (C16), 129.3 (C9), 129.1 (C11), 129.0 (C18), 128.9 (C8), 127.1 (C10), 67.0 (C5), 55.5 (C4), 51.9 (C21), 45.9 (C13), 38.3 (C6).

Computational details. The geometry of the molecules has been fully optimized with the hybrid HF/DFT B3LYP[32] computational method and the 6-31G(d) basis set.[33] Frequency calculations have been carried out at the same computational level to verify that the structures obtained correspond to energetic minima. A further optimization has been carried out at the B3LYP/6-311++G(d,p) level.[34] These geometries have been used for the calculations of the absolute chemical shieldings with the GIAO method[35] and the B3LYP/6-311++G(d,p) computational level. All the calculations have been carried out with the Gaussian-09 package.[36] The following equations have been used to transform absolute shieldings into chemical shifts:

$$\delta^1H = 31.0 - 0.97 \times \sigma^1H \quad (1)$$

(reference TMS, 0.00 ppm).[37]

$$\delta^{13}C = 175.7 - 0.963 \times \sigma^{13}C \quad (2)$$

(reference TMS, 0.00 ppm).[38]

$$\delta^{15}N = -152.0 - 0.946 \times \sigma^{15}N \quad (3)$$

(reference ext. neat $MeNO_2$, 0.00 ppm).[38]

Crystal structure determination. Suitable crystals for X-ray diffraction experiments were obtained by crystallization of **5** in a mixture of hexane/ethyl acetate.

A crystal from compound **5** was used for data collection at 100 K using CuK/α, λ=1.54184 Å. A total of 47,287 ($-8\leq h\leq 8$, $-39\leq k\leq 39$, $-33\leq l\leq 33$) reflections were collected with 23,654 independent reflections. Data collection was made using the program CrysAlis CCD.[26] An analytical numeric absorption correction[27] was applied to the intensity data.

Crystal structure was solved by Direct Methods, using the program Sir2002.[28] Anisotropic least-squares refinement was carried out with SHELXL-97.[29] Refinement was made in the space group $P2_1$. Further details of the X-ray structural analysis are given in Table 3. Hydrogen bonds are listed in Table 4. Geometrical calculations were made with PARST97[30] and molecular graphics with ORTEP-3[31] for Windows.

The Platon ADDSYM check results are the following:

Transformation matrix for cell and HKL data.

The following crystal structure has been deposited at the Cambridge Crystallographic Data Centre and allocated the deposition number: CCDC 835633. Copies of the data can be obtained, free of charge, on application to CCDC, 12 Union Road, Cambridge CB2 1EZ, UK, (fax: +44 (0)1223 336033 or e-mail: deposit@ccdc.cam.ac.uk).

Acknowledgements

This work was supported by the Ministerio de Ciencia e Innovación (Project No. CTQ2009-13129-C02-02), Comunidad Autónoma de Madrid (Project MADRISOLAR, ref. S-0505/PPQ/0225), SAF2009-12422-C02-02, and RTA (RED Trastornos Adictivos RD06/001/0014). The authors thank the CTI (CSIC) for allocation of computer time and the Departamento de Química Orgánica y Bioorgánica (UNED) for recording the CPMAS NMR spectra. Financial support from Spanish Ministerio de Ciencia e Innovación (MAT2006-01997, MAT2010-15094 and 'Factoría de Cristalización' Consolider Ingenio 2010), and FEDER funding is acknowledged.

References and notes

1. Brickner, S. J.; Hutchinson, D. K.; Barbachyn, M. R.; Manninen, P. R.; Ulanowicz, D. A.; Garmon, S. A.; Grega, K. C.; Hendges, S. K.; Toops, D. S.; Ford, C. W.; Zurenko, G. E. *J. Med. Chem.* **1996**, *39*, 673.
2. Zappia, G.; Gacs-Baitz, E.; Delle Monache, G.; Misiti, D.; Nevola, L.; Botta, B. *Curr. Org. Synth.* **2007**, *4*, 81.
3. Evans, D. A.; Bartroli, J.; Shih, T. L. *J. Am. Chem. Soc.* **1981**, *103*, 2127.
4. Masamune, S.; Choy, S.; Kerdesky, W.; Imperiali, F. A. J. *J. Am. Chem. Soc.* **1981**, *103*, 1566.
5. Evans, D. A.; Ennis, M. D.; Mathre, D. J. *J. Am. Chem. Soc.* **1982**, *104*, 1737.
6. Miyachi, H.; Nomura, M.; Tanase, T.; Takahashi, Y.; Ide, T.; Tsunoda, M.; Murakami, K.; Awano, K. *Bioorg. Med. Chem. Lett.* **2002**, *12*, 77.
7. Nomura, M.; Tanase, T.; Miyachi, H. *Bioorg. Med. Chem. Lett.* **2002**, *12*, 2101.
8. Bull, S. D.; Davies, S. G.; Jones, S.; Sanganee, H. J. *J. Chem. Soc., Perkin Trans. 1* **1999**, 387.
9. The same results were obtained when oxazolidinone **2** was employed instead of **1** obtaining **4** (*S*, *R*) as major compound (60% yield) that was characterized by mass spectrometry: *m*/*z*: 274 (100%) $[M+H]^+$. Analysis of the enantiomeric excess, 95%, was performed by HPLC with a CHIRAPAC OD column (0.0046×0.25 mm, flow rate 1.00 mL/min, UV 254 nm, hexane/*i*-PrOH.
10. (a) Barfield, M.; Chakrabarti, B. *Chem. Rev.* **1969**, *69*, 757 (see p 763); (b) Tormena, C. F.; Freitas, M. P.; Rittner, R.; Abraham, R. J. *Magn. Reson. Chem.* **2002**, *40*, 279; (c) Kamienska-Trela, K.; Wojcik, J. Applications of Spin–Spin Couplings In *Nuclear Magnetic Resonance*; Webb, G. A., Ed.; Specialist Periodical Reports; Royal Society of Chemistry: Cambridge, 2005; Vol. 34; Chapter 5, p 193.
11. (a) See Ref. 10a (see p 776). (b) Froimowitz, M.; DiMeglio, C. M.; Makriyannis, A. *J. Med. Chem.* **1992**, *35*, 3085; (c) Novak, A.; Bezensek, J.; Groselj, U.; Golobic, A.; Stanovnik, B.; Svete, J. *ARKIVOC* **2011**, *vi*, 18.
12. Bongini, A.; Cardillo, G.; Orena, M.; Porzi, G.; Sandri, S. *Tetrahedron* **1987**, *43*, 4377.
13. Ciclosi, M.; Fava, C.; Galeazzi, R.; Orena, M.; González-Rosende, M. E.; Sepúlveda-Arques, J. *Tetrahedron: Asymmetry* **2004**, *15*, 1937.
14. Tomasini, C.; Angelici, G.; Castellucci, N. *Eur. J. Org. Chem* **2011**, *20–21*, 3648.
15. (a) Karplus, M. *J. Chem. Phys.* **1959**, *30*, 11; (b) Karplus, M. *J. Phys. Chem.* **1960**, *64*, 1793; (c) Karplus, M. *J. Am. Chem. Soc.* **1963**, *85*, 2870; (d) Emsley, J. W.; Feeney, J.; Sutcliffe, L. H. *High Resolution Nuclear Magnetic Resonance Spectroscopy*; Pergamon: Oxford, 1965; Vol. 2; 678.
16. Haasnoot, C. A. G.; DeLeeuw, F. A. A. M.; Altona, C. *Tetrahedron* **1980**, *36*, 2783.
17. (a) Elguero, J.; Fruchier, A. *An. Quim.* **1974**, *70*, 141; (b) Jimeno, M. L.; Elguero, J.; Carmona, D.; Lamata, M. P.; San José, E. *Magn. Reson. Chem.* **1996**, *34*, 42; (c) Alkorta, I.; Elguero, J. *Org. Biomol. Chem.* **2003**, *1*, 585; (d) Alkorta, I.; Elguero, J. *Int. J. Mol. Sci.* **2003**, *4*, 64; (e) Alkorta, I.; Elguero, J. *Theor. Chem. Acc.* **2004**, *111*, 31; (f) Del Bene, J.; Elguero, J. *J. Phys. Chem. A* **2006**, *110*, 12543.
18. Navarro-Vázquez, A.; Cobas, J. C.; Sardina, F. J.; Casanueva, J.; Díez, E. *J. Chem. Inf. Comput. Sci.* **2004**, *44*, 1680.
19. Llamas-Saíz, A.; Foces-Foces, C.; Sobrados, I.; Elguero, J.; Meutermans, W. *Acta Crystallogr., Sect. C* **1993**, *49C*, 724.
20. Yap, G. P. A.; Claramunt, R. M.; López, C.; García, M. A.; Pérez-Medina, C.; Alkorta, I.; Elguero, J. *J. Mol. Struct.* **2010**, *965*, 74.
21. 'The use of PPAR-alpha/gamma dual agonists for the treatment of metabolic syndromes', Expert Opinion on Therapeutic Patents, 2004, 14, 1797.
22. Kumar, S.; Tan, E. Y.; Hartmann, G.; Biddle, Z.; Bergman, A. J.; Dru, J.; Ho, J. Z.; Jones, A. N.; Staskiewicz, S. J.; Braun, M. P.; Karanam, B.; Dean, D. C.; Gendrano, I. N.; Graves, M. W.; Wagner, J. A.; Krishna, R. *Drug Metab. Dispos.* **2010**, *38*, 474.
23. Smith, C. J.; Ali, A.; Hammond, M. L.; Li, H.; Lu, Z.; Napolitano, J.; Taylor, G. E.; Thompson, C. F.; Anderson, M. S.; Chen, Y.; Eveland, S. S.; Guo, Q.; Hyland, S. A.; Milot, D. P.; Sparrow, C. P.; Wright, S. D.; Cuminskey, A.-M.; Latham, M.; Peterson, L. B.; Rosa, R.; Pivnichny, J. V.; Tong, X.; Xu, S. S.; Sinclair, P. J. *J. Med. Chem.* **2011**, *54*, 4880.
24. gNMR5.0, IvorySoft, AmorWay, Letchworth, Herts.SG61ZA, United Kingdom, 2004.
25. Press, W. H.; Teukolsky, S. A.; Vetterling, W. T.; Flannery, B. P. *Numerical Recipes in C: The Art of Scientific Computing*, 2nd ed.; Cambridge University: Cambridge, 1992, pp 994.
26. *Oxford Diffraction. CrysAlis CCD, CrysAlis RED and CrysAlis PRO*; Oxford Diffraction Ltd: Yarnton, England, 2009.
27. Clark, R. C.; Reid, J. S. *Acta Crystallogr., Sect. A* **1995**, *A51*, 887.
28. SIR2002- Burla, M. C.; Camalli, M.; Carrozzini, B.; Cascarano, G. L.; Giacovazzo, C.; Polidori, G.; Spagna, R. *J. Appl. Crystallogr.* **2003**, *36*, 1103.
29. Sheldrick, G. M. *SHELXL-97* A computer program for refinement of crystal structures; University of Göttingen: Göttingen, 1997.
30. Nardelli, M. *Comput. Chem.* **1983**, *7*, 95.
31. Farrugia, L. J. *J. Appl. Crystallogr.* **1997**, *30*, 565.
32. (a) Becke, A. D. *Phys. Rev. A: At., Mol., Opt. Phys.* **1988**, *38*, 3098; (b) Becke, A. D. *J. Chem. Phys.* **1993**, *98*, 5648; (c) Lee, C.; Yang, W.; Parr, R. G. *Phys. Rev. B: Condens. Matter* **1988**, *37*, 785.
33. Hariharan, P. A.; Pople, J. A. *Theor. Chim. Acta* **1973**, *28*, 213.
34. (a) Ditchfield, R.; Hehre, W. J.; Pople, J. A. *J. Chem. Phys.* **1971**, *54*, 724; (b) Frisch, M. J.; Pople, J. A.; Binkley, J. S. *J. Chem. Phys.* **1984**, *80*, 3265.
35. (a) Ditchfield, R. *Mol. Phys.* **1974**, *27*, 789; (b) London, F. *J. Phys. Radium* **1937**, *8*, 397.
36. Frisch, M. J.; Trucks, G. W.; Schlegel, H. B.; Scuseria, G. E.; Robb, M. A.; Cheeseman, J. R.; Montgomery, J. A., Jr.; Vreven, T.; Kudin, K. N.; Burant, J. C.; Millam, J. M.; Iyengar, S. S.; Tomasi, J.; Barone, V.; Mennucci, B.; Cossi, M.; Scalmani, G.; Rega, N.; Petersson, G. A.; Nakatsuji, H.; Hada, M.; Ehara, M.; Toyota, K.; Fukuda, R.; Hasegawa, J.; Ishida, M.; Nakajima, T.; Honda, Y.; Kitao, O.; Nakai, H.; Klene, M.; Li, X.; Knox, J. E.; Hratchian, H. P.; Cross, J. B.; Adamo, C.; Jaramillo, J.; Gomperts, R.; Stratmann, R. E.; Yazyev, O.; Austin, A. J.; Cammi, R.; Pomelli, C.; Ochterski, J. W.; Ayala, P. Y.; Morokuma, K.; Voth, G. A.; Salvador, P.; Dannenberg, J. J.; Zakrzewski, V. G.; Dapprich, S.; Daniels, A. D.; Strain, M. C.; Farkas, O.; Malick, D. K.; Rabuck, A. D.; Raghavachari, K.; Foresman, J. B.; Ortiz, J. V.; Cui, Q.; Baboul, A. G.; Clifford, S.; Cioslowski, J.; Stefanov, B. B.; Liu, G.; Liashenko, A.; Piskorz, P.; Komaromi, I.; Martin, R. L.; Fox, D. J.; Keith, T.; Al-Laham, M. A.; Peng, C. Y.; Nanayakkara, A.; Challacombe, M.; Gill, P. M. W.; Johnson, B.; Chen, W.; Wong, M. W.; Gonzalez, C.; Pople, J. A. *Gaussian 03*; Gaussian: Pittsburgh PA, 2003.
37. Silva, A. M. S.; Sousa, R. M. S.; Jimeno, M. L.; Blanco, F.; Alkorta, I.; Elguero, J. *Magn. Reson. Chem.* **2008**, *46*, 859.
38. Blanco, F.; Alkorta, I.; Elguero, J. *Magn. Reson. Chem.* **2007**, *45*, 797.